Measurement of Electron Density and Temperature in a Pulsed Argon Ion Laser

By

Takashi FUJIMOTO*, Yoshiro OGATA*
and Kuniya FUKUDA*

(Received January 8, 1970)

This paper is concerned with some results of experiment and analysis on plasma of pulsed argon ion laser. A long pulsed discharge was brought about with varied discharge voltages of 2~5 kV at pressures from 10 to 100 m Torr. Laser oscillations of 6 argon ion lines were observed in the pressure range from 10 to 30 m Torr. The change of electron density during the discharge was measured with a He-Ne laser interferometer and a double probe, giving the value of the order of $10^{14}\,\text{cm}^{-3}$ for the above discharge conditions. The time variation of electron temperature was also determined with a double probe and by the measurement of plasma electrical resistivity. Temperature of $4.5\sim7\times10^4\,°\text{K}$ was obtained. From the analysis of the measured plasma parameters it is concluded that the free fall model of Tonks-Langmuir is valid in the laser plasma except in the early period of the pulsed discharge. Further, observed laser oscillations and spontaneous emissions are analized and three-level model is supported for the pumping of excited levels of argon ion lines in the quasi-CW oscillation region, i.e. the later period, of the laser discharge.

1. Introduction

Since the first argon ion laser oscillation was reported, many experimental and theoretical investigations have been carried out to clarify the mechanism of the oscillation and the following three models of pumping have been proposed.

i) Four level model[1]: neutral atom in ground state is directly excited to one of the laser upper levels of ion with a single electronic collision;

$$\text{Ar}(3\,\text{p}^6)+\text{e} \longrightarrow \text{Ar}^+(3\,\text{p}^4, 4\,\text{p})+2\text{e}. \qquad (1)$$
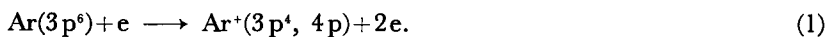
ii) Three level model[2]: the laser upper levels are pumped from the ground state of ion;

$$\text{Ar}^+(3\,\text{p}^5)+\text{e} \longrightarrow \text{Ar}^+(3\,\text{p}^4, 4\,\text{p})+\text{e}. \qquad (2)$$

* Department of Mechanical Engineering, II.

iii)   Neutral atoms Ar* in metastable or higher excited states are responsible for the pumping of the laser upper levels[3];

$$Ar^*(3p^5, \ 4s)+e \longrightarrow Ar^+(3p^4, \ 4p)+2e. \tag{3}$$
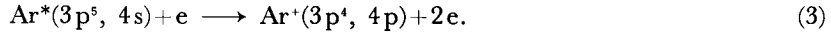
The second model with some modifications has been applied to explain some phenomena of the CW oscillation qualitatively.   On the other hand, pulsed oscillation is less understood although many observations have been reported.   It seems that plasma parameters, such as electron density, electron temperature, neutral particle density, plasma potential and so on, constitute the essential condition for the laser oscillation.   Some authors have determined these parameters experimentally and theoretically, but disagreement among them still remains[4]-[12].

In the present experiment quasi-CW oscillation of argon ion laser was brought about in the later period of long pulsed discharge.   Electron density as well as temperature were determined by using two different methods so that the data could be checked with each other; electron density was measured with a He-Ne laser interferometer and a double probe, and electron temperature with a double probe and also by measuring plasma electrical resistivity.   The analysis of these data leads to the conclusion that the free fall model proposed by Tonks and Langmuir is valid for the argon laser plasma in the later period of the pulsed discharge.   The results of measured electron density and temperature are compared with those of other authors.

The behavior of side light emissions was also observed and discussed in relation to those of electron density and temperature of the pulsed laser plasma. The results support the three-level model of pumping in the discharge period of quasi-CW oscillation.

2.   Experimentals

A laser tube used in the present experiment was 8mm in inner diameter and 72cm in active discharge length.   It had Brewster windows and a cold activated cathode.   A capacitor of $C=20\,\mu F$ with voltage V of 2~5 kV is discharged through the laser tube with $10\,\Omega$ series resistor, giving maximum current of $i=200\sim500$ A. Initial gas pressure p was varied from 12 to 30 mTorr.   A nearly confocal cavity was formed with dielectric mirrors of high reflectivities, 98 % and 99.7 %.   Under these conditions 6 laser lines (4579 Å~5145 Å) oscillated.   The oscillations for three lines of 4765 Å, 4880 Å and 5145 Å are shown for some discharge conditions in Fig. 1.   These oscillations correspond to the second oscillation peak, which has been observed after the initial oscillation peak of very short duration in pulsed laser experiment[13]-[15].   Saturation of the oscillation peaks is seen against increase
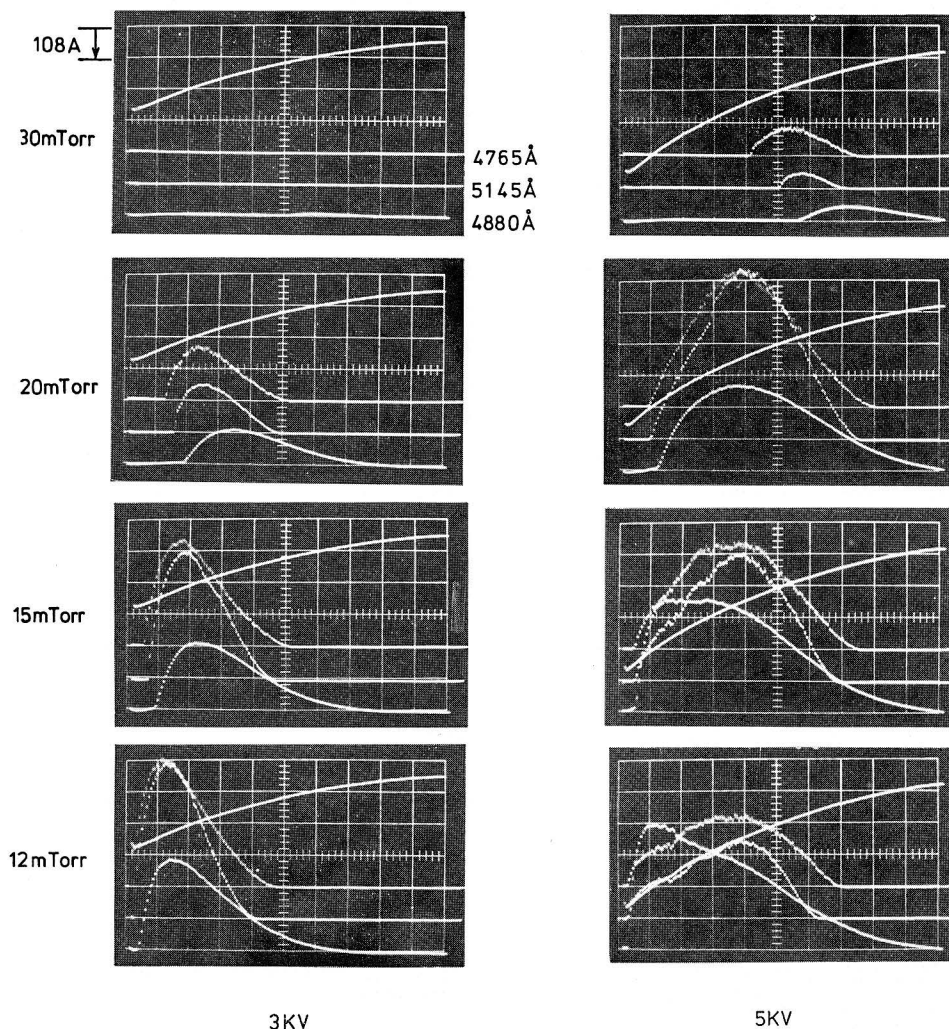
Fig. 1. Discharge current and laser oscillations at pressures of 30, 20, 15 and 12 mTorr for discharge voltages of 3 and 5 kV. Current is to be measured downward from the top scale line (108 A/div.). Oscillations are shown for 4765 Å, 5145 Å and 4880 Å. Sweep rate is 50 μ sec/div.

in discharge current for a given pressure except in the case of 4880 Å.

Temporally resolved data of electron density during discharge were obtained with a coupled cavity, spherical He-Ne laser interferometer[16], in which 6328 Å oscillation was used. The argon laser tube was located in the reference cavity, as shown in Fig. 2. Owing to a high reflectivity (99.7%) of the mirror M_2 and slight losses at the windows of the discharge tube, the change in Q-value of the reference cavity produced no appreciable effect on the output power of the He-Ne laser. Inter-
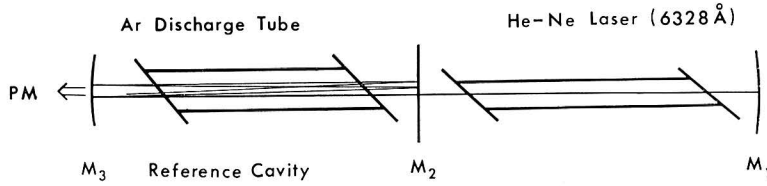
Ar Discharge Tube   He—Ne Laser (6328 Å)

PM

M_3 Reference Cavity M_2 M_1

Fig. 2. Schematic diagram of the optical system. PM : photomultiplier, M_1 and M_3: spherical mirrors, M_2: plane mirror with reflectivity of 99.7 %.

ference fringes were observed on the transmitted light through the reference cavity with a photomultiplier. For a homogeneous plasma of L cm in length, the change in electron density Δn_e, necessary to produce a full cycle of modulation on the transmitted light, is

$$\Delta n_e = \frac{1.12 \times 10^{17}}{sL\lambda_0} \text{ cm}^{-3} \text{ cycle}^{-1}, \tag{4}$$

where s is a sensitivity factor and λ_0 is the wavelength (in micron) of the sensing He-Ne laser beam. As is verified later, atom density is comparable to electron or ion density, so that the contributions of atoms and ions to the plasma refractivity can be neglected in comparison with that of electrons. For the sensitivity factor of

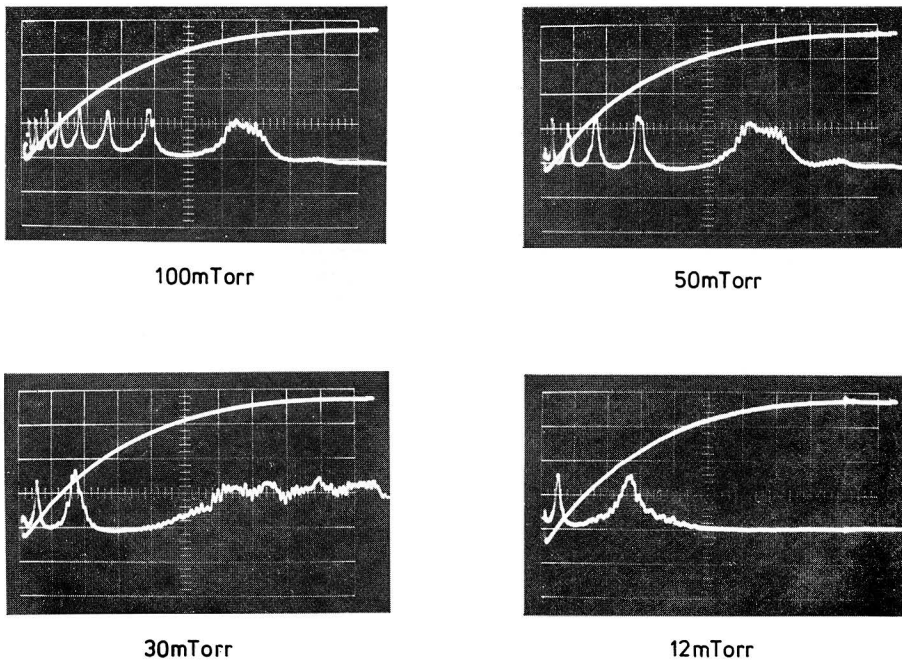100mTorr

50mTorr

30mTorr

12mTorr

Fig. 3. Observed interference fringes and discharge currents for $V=5$ kV discharges. Pressure is 100, 50, 30 and 12 mTorr. Sweep rate is 0.1 m sec/div.

$s=7$ and the plasma length of $L=72$ cm, Eq. (4) gives the increase (or decrease) of electron density $\Delta n_e = 3.5 \times 10^{14}$ cm^{-3} for one fringe jump. A bundle of sensing laser beams was aligned to pass through a cross sectional area of 1 mm $\times$ 3 mm along the axis of the argon discharge tube, so that the electron density $(n_e{}^0)$ could be observed on the tube axis.

Fig. 3 shows the fringe jumps produced by the laser discharges ($p=12$ and 30 m Torr, $V=5$ kV) and the discharges at higher pressures ($p=50$ and 100 mTorr, $V=5$ kV), where the latter did not give rise to the laser oscillation. In each figure
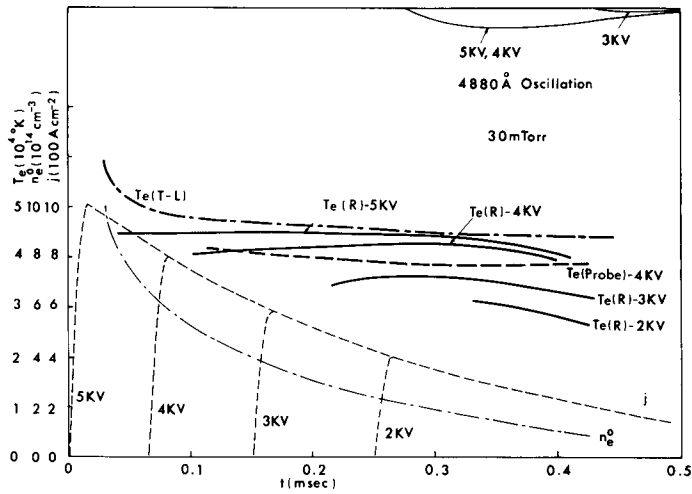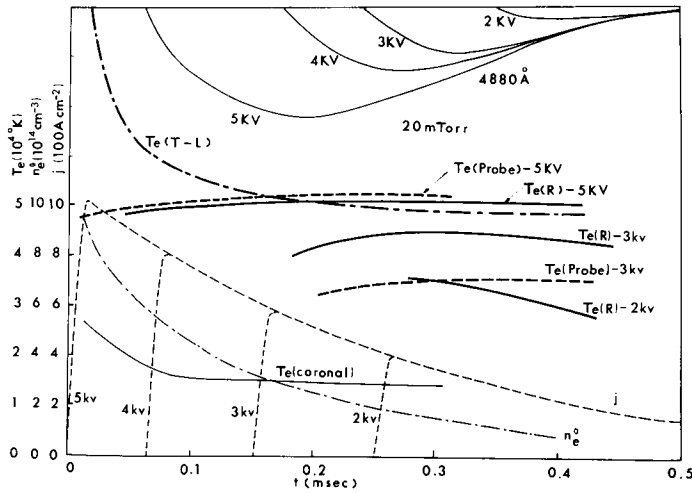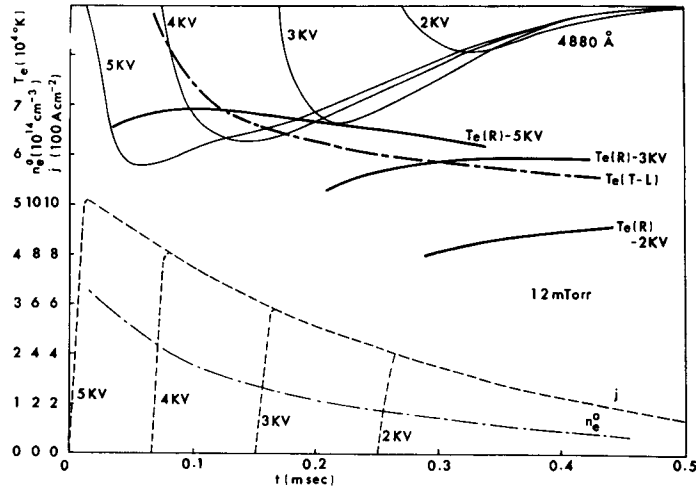
Fig. 4 (a)

Fig. 4 (b)

Fig. 4 (c)

Fig. 4. Time variations of 4880 Å oscillations, electron temperatures, electron
densities and discharge current densities for varied discharge voltages from
2 to 5 kV. Pressure is 30 mTorr in (a), 20 mTorr in (b) and 12 mTorr
in (c). 4880 Å oscillations are to be seen downward from the top scale
line. $T_e(R)$ and $T_e(Probe)$ are determined from the measured electrical
resistivity and with the double probe method, respectively. $T_e(T\text{-}L)$ and
$T_e(coronal)$ are calculated from the plasma theory by Tonks-Langmuir
and the coronal equilibrium, respectively.

fringe jump due to the initial rise of discharge current is not seen, which corresponds
to the very fast increase of electron density, and the observed fringe jump is
considered to correspond to the gradual decrease of electron density during the
decaying discharge current. Observed electron densities $n_e{}^0$ are shown for $p=30$,
20 and 12 mTorr in Fig. 4 (a), (b) and (c), respectively, and plotted as a function
of discharge current density in Fig. 5. This figure indicates that the electron
density curves can be smoothly extended with straight lines (dashed lines) and
hence the electron density is proportional to the discharge current in the low
current region.

Electron density was also measured by the double probe method[17]. Two
probes of tungsten wire, 0.2 mm in diameter and 1.5 mm in length, were inserted into
the discharge tube. They were set opposite each other, leaving a space of 2 mm
between their tops. Ion mean free path $\lambda_i = 1/n\sigma$ is determined from the cross
section σ for momentum transfer collision with neutral particles[18], where n is neutral
particle density. The values of $\sigma = 10^{-14} \sim 10^{-15}$ cm² [19]-[21] lead to the λ_i-values of
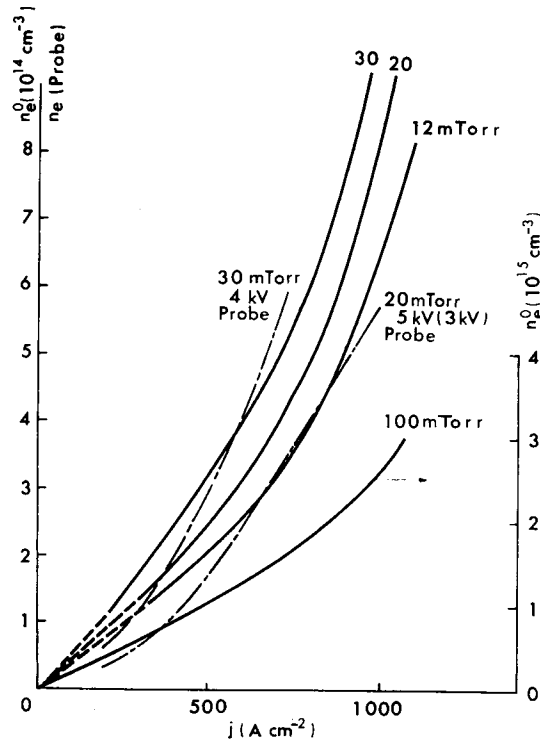$0.1 \sim 1$ cm in the present laser discharge. Therefore, the effect of quasi-neutral

Fig. 5.   Electron densities of $n_e{}^0$ and $n_e(Probe)$ versus discharge
current density for varied pressures.   The curve for 100mTorr
is referred to the ordinate in the right hand side.

plasma region on probe ion current must be taken into account[22].   Probe current data were analyzed under this condition.   The results, which are presented in Fig. 5 as $n_e(Probe)$, are in fairly good agreement with those of the interferometric measurement.

Electron temperature was measured by two methods, that is, the double probe method and the measurement of plasma electrical resistivity.   Examples of the temperature with the double probe measurement, $T_e(Probe)$, are shown in Figs. 4 (a) and (b) (dahed lines).

Axial potential gradient of plasma was measured with two probes, which were inserted 26 cm apart in the discharge tube, and the observed potential was corrected for "contact potential difference" between plasma and probe with the aid of the double probe data.   Then electrical resistivity of plasma was readily determined from current density, and together with the measured electron density, it was applied to Spitzer's formula[23] of electrical resistivity η;

$$\eta = 6.53 \times 10^3 \frac{\ln A}{T_e^{3/2}} \text{ cm } \Omega, \tag{5}$$

with

$$A = \frac{3}{2e^3} \left(\frac{k^3 T_e^3}{\pi n_e} \right)^{1/2}. \tag{6}$$

This procedure gave the electron temperatures $T_e(R)$ shown in Figs. 4 (solid lines). The application of Spitzer's formula is justified because the rate of collisional momentum transfer of electrons to neutral atoms is negligible compared with that to ions. In Figs. 4 one can see that the electron temperature varies only slightly during the discharge.

Figs. 4 (a), (b) and (c) show discharge current density j, electron density on the tube axis n_e^0, temperatures, $T_e(Probe)$ and $T_e(R)$, and 4880 Å laser oscillation for various discharge voltages V at the pressures of $p=30$, 20 and 12 mTorr, respectively. Discharge currents showed the same exponential decay for the discharges with different voltages and so in Figs. 4 the time origins are shifted for the discharges with $V=4$, 3 and 2 kV in such a way that the current density in each case coincides with that of the discharge with $V=5$ kV.

3. Discussions

In order to know the "state" of the pulsed argon laser plasma, the following two models are presented for ionization and recombination. Here it is assumed that double ionization is small[12] and plasma is quasi-steady. In the following discussions the data of electronic collision cross sections and rate coefficients are taken from Drawin's report[24].

i) Collisional-radiative model[25] : If the effect of tube wall is neglected, collisional-radiative ionization-recombination theory can be applied, so that electron temperature is determined from measured electron density.

A balance equation for ionization and recombination can be written by

$$n n_e S(T_e) = n_i n_e \alpha(T_e), \tag{7}$$

where n_e and n_i are electron and ion densities, respectively, and S and α are collisional-radiative ionization and recombination coefficients, respectively. In the low electron density limit for optically thin plasma (coronal equilibrium), S and α are simply collisional ionization and radiative recombination coefficients, respectively. Then n and $n_i(=n_e^0)$ determine* the ratio of $S(T_e)/\alpha(T_e)$ and hence

---

* Axial drift velocity of ion has been measured to be about 10^4 cm sec^{-1} [5],[10]. With this velocity ion moves at most 10 cm in our discharge duration, and so the "drive out" of gas particles can be neglected.

electron temperature, which is shown in Fig. 4 (b) as $T_e(coronal)$ (solid line). In the actual plasma with electron density of $n_e = 10^{14} \sim 10^{15}$ cm^{-3} the values of S and α deviate from those in the coronal limit and then they will give a lower temperature than $T_e(coronal)$.

ii) Free fall model by Tonks and Langmuir[26] : As is mentioned in section 2, mean free path of ion is of the order of mm, comparable with the tube radius, and the free fall model can be applied[27],[28]. According to this model, plasma potential is formed between the tube center and the wall, the difference of which is nearly equal to the energy corresponding to the electron temperature. Ion runs freely in this plasma potential to the tube wall and recombines there, volume recombination being neglected. Then a balance equation is given by

$$n\, n_e S(T_e) = 5.5 \times 10^2 n_e^0 T_e^{1/2} \tag{8}$$

instead of Eq. (7), where n_e^0 is the electron density at the tube center. The right hand side of Eq. (8) represents the positive ion current to the tube wall. Here average electron density n_e is given by $0.7 \times n_e^0$. Therefore, the neutral particle density in plasma determines electron temperature, which is shown in Figs. 4 as $T_e(T\text{-}L)$ (broken lines).

Temperature $T_e(coronal)$ does not give a reasonable value, whereas $T_e(T\text{-}L)$ gives good agreement with the measured values of $T_e(R)$ and $T_e(Probe)$ except in
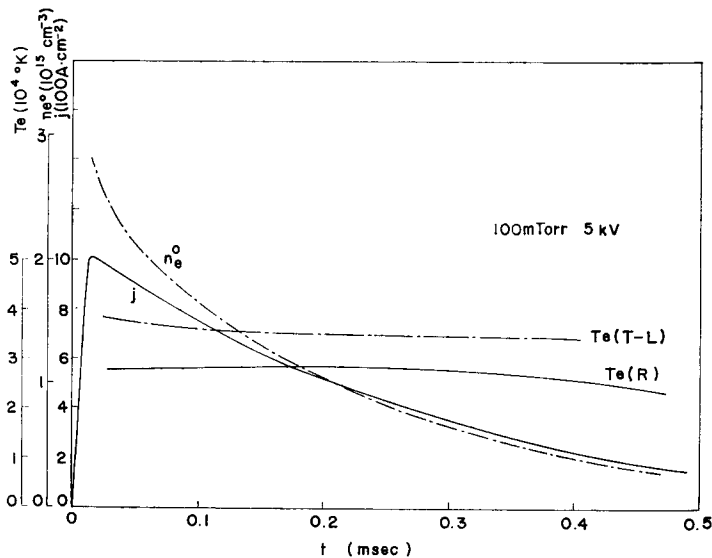

Fig. 6. Observed electron density n_e^0 and temperature $T_e(R)$, and calculated temperature $T_e(T\text{-}L)$. Pressure is 100 mTorr and discharge voltage is 5 kV.

the early period of discharge (Figs. 4). This result supports the conclusion that the free fall model describes correctly the laser plasma at the later period of $V=5$ kV discharge. The disagreement in the early period of discharge may be due to the fact that Tonks-Langmuir theory can not essentially be applied to high-current-discharge plasma with high ionization ratio. Also $T_e(T\text{-}L)$ fails to give an agreement with the measured value of electron temperature $T_e(R)$ for the discharge at $p=100$ mTorr (Fig. 6). This is considered to be caused by the breakdown of the assumption that ion mean free path is longer than or comparable with the tube radius[27]. It is not clear why plasmas have lower temperatures of $T_e(R)$ or T_e (*Probe*) than $T_e(T\text{-}L)$ for the discharges with lower voltages (Figs. 4).

For given temperatures in Figs. 4, the ionization relaxation time, $\tau_{\text{ion}}=1/n\,S(T_e)$, is of the order of μ sec, which is much shorter than the decay time of plasma, and so the plasma is considered to be quasi-steady.

The emission intensities of 4880 Å laser oscillations in Fig. 4 (b) ($p=20$ mTorr) are plotted as a function of discharge current in Fig. 7. The time decays of the oscillations for $V=3$, 4 and 5 kV fall into a straight line, and this "linear" relation to discharge current has been observed in the CW oscillation[2,7,29,30]. The same linear relation holds for the discharges at 15 mTorr. This fact indicates that the oscillation of the "linear" part in Fig. 7 is in CW mode; that is, quasi-CW oscillation begins at about 300 μ sec after the beginning of the discharge in the case of $V=5$ kV
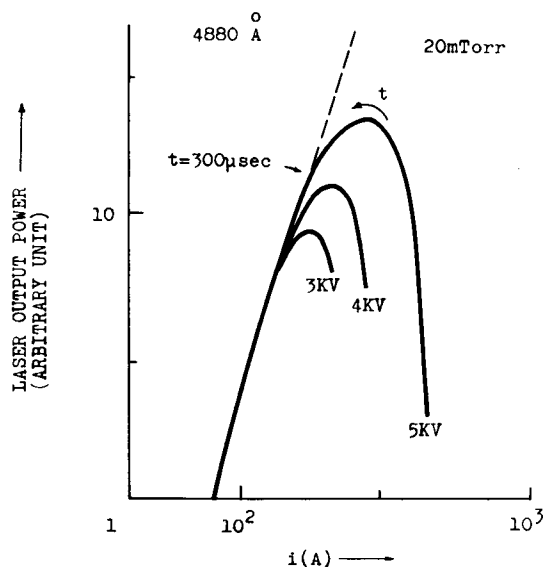

Fig. 7. 4880 Å laser oscillations versus discharge current. Pressure is 20 mTorr.
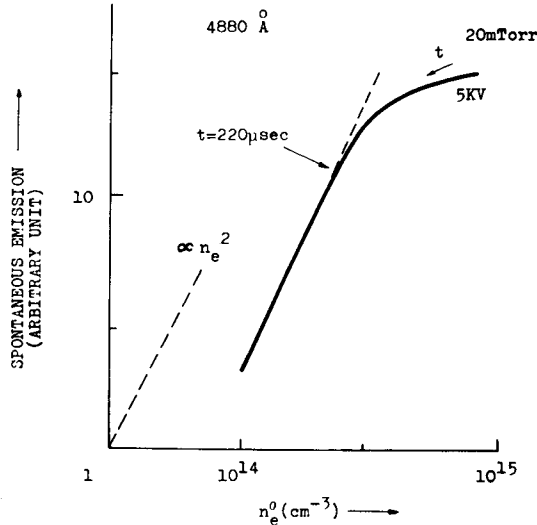
Fig. 8.   4880 Å spontaneous emission versus electron density.   Pressure
          is 20 mTorr and discharge voltage is 5 kV.

discharge.

For the discharge with $V=5$ kV (Fig. 1), the oscillations at $p=30$ mTorr are much weaker than those at 20 mTorr, while the discharges at 15 and 12 mTorr give rise to unstable natures of plasma potential, probe current and laser oscillation, and the oscillations themselves become also weaker.   It follows that the laser oscillation at $p=20$ mTorr is in the optimum condition for quasi-CW mode. Plasma parameters in this condition are shown in Table 1.

The values of electron temperature, either determined by Kitaeva et al.[4]−[6] and calculated by Zarowin[9], are in fairly good agreement with the present data.

On the other hand, Zarowin[9] showed larger values of electron density by one order of magnitude in comparison with those of the present data.   The values obtained by Bennett et al.[10],[11] at low-current density are larger than ours by a

Table 1   Discharge current density j, electron temperature $T_e(=$
          $T_e(R)=T_e$ $(Probe)=T_e$ $(T\text{-}L))$, average electron density n_e,
          and neutral particle density n in the quasi-CW oscillation for
          5 kV discharge at 20 mTorr.   For $j \leq 300$ A cm^{-2}, quasi-CW
          is established.

j(A cm^{-2})	T_e(10^4 °K)	n_e(10^{14} cm^{-3})	n(10^{14} cm^{-3})
120	5.0	0.3	6.8
250	5.0	0.7	6.4
300	5.0	0.9	6.2
500	5.0	1.8	5.3

factor of 4. Kitaeva et al.[4]−[6] presented smaller values by a factor and, furthermore, their results are insensitive to the discharge current, in contrast with the present results. Also Levinson et al.[12] reported smaller values by a factor of 3. Borizova et al.[8] presented the value of $5 \times 10^{13} \mathrm{cm}^{-3}$ at low-current density $(j=200 \mathrm{~A~cm}^{-2})$, which is in good agreement with the present data.

Side light spontaneous emissions of several ion lines with upper levels of 4p, 4d and 5s were observed and plotted as a function of electron density. One example is shown for 4880 Å emission (with the upper level of $4\mathrm{p}^2\mathrm{D}_{5/2}$) in the case of $p=20$ mTorr and $V=5$ kV in Fig. 8. The quadratic dependence of the emission on electron density is seen in the later period of discharge. This relation is also seen for other emission lines.

Since the electron temperature is almost constant throughout the discharge, the above result suggests that the pumping of the excited levels of argon ion is proportional to either electron or ion densities. Therefore, the three level model of Eq. (2) is supported for the pumping mechanism in the period of quasi-CW oscillation for the pulsed discharge.

Further experiment and analysis on atomic process in the laser plasma are now in progress. The results will be reported in the near future.

References

1) W. R. Bennett Jr., J. W. Knutson Jr., G. N. Mercer and J. L. Detsch; Appl. Phys. Letters, **4**, 180 (1964).
2) E. F. Labuda, E. I. Gordon and R. C. Miller; IEEE J. Quant. Electr., **QE-1**, 273 (1965).
3) W. R. Bennett Jr. and W. Lichten; Appl. Optics Suppl. 2, 3 (1965).
4) V. F. Kitaeva, Yu. I. Osipov and N. N. Sobolev; JETP Letters, **4**, 146 (1966).
5) V. F. Kitaeva, Yu. I. Osipov and N. N. Sobolev; IEEE J. Quant. Electr., **QE-2**, 635 (1966).
6) V. F. Kitaeva, Yu. I. Osipov, P. L. Rubin and N. N. Sobolev; IEEE J. Quant. Electr., **QE-5**, 72 (1969).
7) G. Herziger and W. Seelig; Zeit. Phys., **215**, 437 (1968), Zeit. Phys., **219**, 5 (1969).
8) M. S. Borisova, Ye. F. Ichenko, M. V. Ladygin, M. A. Molchashkin, Ye. F. Nasedkin and G. S. Ramazanova; Radio Eng. and Elec. Phys., **12**, 529 (1967).
9) C. B. Zarowin; Appl. Phys. Letters, **15**, 36 (1969).
10) E. A. Ballik, W. R. Bennett Jr. and G. N. Mercer; Appl. Phys. Letters, **15**, 214 (1966).
11) G. H. Mercer, V. P. Chebotayev and W. R. Bennett Jr.; Appl. Phys. Letters, **10**, 177 (1967).
12) G. R. Levinson, V. F. Papulovskiy and V. P. Tychinskiy; Radio Eng. and Elec. Phys., **13**, 578 (1968).
13) R. K. Leonov, E. D. Protsenko and Yu. M. Sapunov; Opt. Spectr., **21**, 141 (1966).
14) W. Demtröder and E. Elendt; Zeit. Naturforschg., **21a**, 2049 (1966).
15) S. Kobayashi, T. Izawa, K. Kawamura and M. Kamiyama; IEEE J. Quant. Electr., **QE-2**, 699 (1966).
16) J. B. Gerardo and J. T. Verdeyen; Proc. IEEE, **52**, 690 (1964).
17) E. O. Johnson and L. Malter; Phys. Rev., **80**, 58 (1950).

18) J. B. Hasted; "Physics of Atomic Collisions" Butterworths Scientific Publications, Ltd., London (1964).

19) E. W. McDaniel; "Collision Phenomina in Ionized Gases" John Wily & Sons, Inc., New York (1964).

20) D. Wobshall, J. R. Graham Jr. and D. P. Malone; Phys. Rev., **131**, 1565 (1963).

21) Yu. M. Kagan and V. I. Perel'; Sov. Phys.—JETP, **2**, 761 (1956).

22) Sin-Li Chen and T. Sekiguchi; J. Appl. Phys., **36**, 2365 (1965).

23) L. Spitzer Jr.; "Physics of Fully Ionized Gases" 2nd. ed., Interscience Publications (1963).

24) H. W. Drawin; Report EUR-CEA-FC-383 (revised) Association-Euratom-C. E. A. (1967).

25) D. R. Bates, A. E. Kingston and R. W. P. McWhirter; Proc. Roy. Soc., **A 267**, 297 (1962).

26) L. Tonks and I. Langmuir; Phys. Rev., **34**, 876 (1929).

27) C. E. Webb; J. Appl. Phys., **39**, 5441 (1968).

28) K. G. Hernqvist and J. R. Fendley; IEEE J. Quant. Electr., **Q E-3**, 66 (1967).

29) E. I. Gordon, E. F. Labuda and W. B. Bridges; Appl. Phys. Letters, **4**, 178 (1964).

30) R. I. Rudko and C. L. Tang; Appl. Phys. Letters, **9**, 41 (1966).